Journal of Solid State Chemistry 182 (2009) 2941–2945

Contents lists available at ScienceDirect

Journal of Solid State Chemistry

journal homepage: www.elsevier.com/locate/jssc

Rapid communication

Synthesis of uniform CdS nanowires in high yield and its single nanowire electrical property

Shancheng Yan [a], Litao Sun [b], Peng Qu [a], Ninping Huang [a], Yinchen Song [a], Zhongdang Xiao [a,*]

[a] State Key Laboratory of Bioelectronics, School of Biological Science and Medical Engineering, Southeast University, Si Pai Lou 2#, Nanjing 210096, PR China
[b] Key Lab of MEMS of Ministry of Education, Southeast University, Si Pai Lou 2#, Nanjing 210096, PR China

ARTICLE INFO

Article history:
Received 12 June 2009
Received in revised form
8 July 2009
Accepted 11 July 2009
Available online 17 July 2009

Keywords:
CdS
Nanowires
Solvothermal
Electrical property

ABSTRACT

Large-scale high quality CdS nanowires with uniform diameter were synthesized by using a rapid and simple solvothermal route. Field emission scan electron microscopy (FESEM) and transmission electron microscopy (TEM) images show that the CdS nanowires have diameter of about 26 nm and length up to several micrometres. High resolution TEM (HRTEM) study indicates the single-crystalline nature of CdS nanowires with an oriented growth along the *c*-axis direction. The optical properties of the products were characterized by UV–vis absorption spectra, photoluminescence spectra and Raman spectra. The resistivity, electron concentration and electron mobility of single NW are calculated by fitting the symmetric *I–V* curves measured on single NW by the metal–semiconductor–metal model based on thermionic field emission theory.

1. Introduction

One-dimensional (1D) semiconductor nanostructures (such as nanotubes, nanorods, nanowires and nanobelts) have recently received considerable attention because of their unique electronic, optical, mechanical properties and their potential applications in nanodevices [1–3]. Among group II–VI semiconductors, CdS with a direct bandgap of 2.42 eV is considered to be an excellent material for various optoelectronic applications in the visible range of the electromagnetic spectrum. Some of these applications include nonlinear optical devices, LEDs, and solar cells [4–6]. Last year, Wang et al. reported CdS NWs can also be used for converting mechanical energy into electricity as ZnO NWs [7,8]. This research further broadens the application of CdS nanowires. Therefore, there have been some reports on the synthesis of 1D CdS nanorods or nanowires with various approaches such as thermal evaporation, chemical vapor deposition and hydrothermal process in the past few years [9–11]. Of the methods used for fabrication of CdS nanomaterials, hydrothermal process has emerged as powerful tools due to some significant advantages, such as cost-effective, controllable particle size, low-temperature and less-complicated techniques [12–14].

In order to evaluate the quality of the semiconducting nanowires, it is best to focus on the electron transport behavior of a single semiconductor nanowire, which is a key issue in understanding the electrical properties of nanowire devices. But vast different results are being obtained from the same type of semiconducting nanowires. If the semiconductor is heavily doped, two electrode contacts may be reduced to ohmic contacts. The result will be a linear *I–V* characteristic [15–17]. On the other hand, if one electrode contact remains Ohmic while the other electrode contact is a Schottky, the result is a rectifying *I–V* characteristic as observed in almost all Schottky diodes by the thermionic emission theory [18]. However, most frequently observed *I–V* characteristic from a semiconducting nanowire is neither linear nor rectifying, while is almost symmetric. Besides, this symmetric *I–V* characteristic cannot be explained by conventional thermionic emission theory. In this work, we have successfully synthesized CdS nanowires via a simple solvothermal route by using $Cd(CH_3COO)_2 \cdot 2H_2O$ as appropriate Cd^{2+} source. The reaction time is reduced to 2 h, comparing to other synthesis which needed long reaction time up to 12 h [19]. In addition, the as-prepared CdS nanowires have more uniform diameter and high yield. More importantly, the *I–V* curve of present single CdS nanowire has a good symmetric characteristic as expected by the theory. The electrical properties of a single CdS nanowire such as resistivity, electron concentration and mobility have been intensively studied based on thermionic field emission theory [20–22].

2. Experimental

The chemicals such as $Cd(CH_3COO)_2 \cdot 2H_2O$ and S powder purchased from Sinopharm Chemical Reagent Co., Ltd. were of analytic grade and used without further purification. The

* Corresponding author. Fax: +86 25 83795635.
E-mail address: zdxiao@seu.edu.cn (Z. Xiao).

0022-4596/$ - see front matter © 2009 Elsevier Inc. All rights reserved.
doi:10.1016/j.jssc.2009.07.016

ethylenediamine was purchased from Shanghai lingfeng Chemical Reagent Co., Ltd. In a typical synthesis procedure, 0.2665 g $Cd(CH_3COO)_2 \cdot 2H_2O$ and 0.0641 g S powder were dissolved in 40 ml ethylenediamine under vigorous stirring and then transferred into a 50 mL Teflon-lined autoclave. The autoclave was heated at 200 °C for 2 h and then cooled to the room temperature. Finally, the resultant sample was filtered off, washed with deionized water, and then dried in a vacuum at 60 °C for 4 h.

The products were characterized by using FESEM (LEO 1550), TEM (JEOL 2100), UV–vis absorption spectra (UV-3150 SHIMADZU), PL spectra (FLS920 F900) and Raman (JY T64000) spectra. The samples used for FESEM observations were supported on the aluminum foil substrate. The samples used for TEM observations were prepared by dispersing some products in anhydrous ethanol followed by ultrasonic vibration for 1 min, then placing a drop of dispersion onto a copper grid. UV–vis absorption spectra were measured by dispersing the sample in anhydrous ethanol at room temperature. PL measurements were conducted at room temperature using the Xe lamp with a wavelength of 350 nm as the excitation source. The Raman spectra were obtained on Raman spectrometers excited by the 514.5 nm line of an Ar^+ laser. The room-temperature electrical transport measurements were done by using a nanoprobe system installed in a TEM. The chemically etched tungsten tips were used as the nanoprobes. The nanoprobe system was connected to a semiconductor characterization system (POWERSUPPLY PSU 100).

3. Results and discussion

The CdS semiconductor nanowires synthesized by the solvothermal method are shown in Fig. 1a. From Fig. 1a, it can be found that the CdS nanowires are of high uniformity and high yield. These nanowires' length is up to several micrometers. The nanowires have diameter of ~26 nm, which is uniform along the entire nanowire length as observed in Fig. 1b. The dark spots on the nanowires in Fig. 1b resulted from the crystallographic defects and overlap of nanowires. The HRTEM images give further insight into the details of the crystal structure of a single nanowire. The clear crystal stripe in the HRTEM image (Fig. 1c) shows that the CdS nanowire is highly crystalline. The distance of interplane perpendicular to the axis direction of the CdS nanowires is 0.338 nm calculated by the software, which is close to the (002) lattice plane of hexagonal CdS suggesting that the CdS nanowires grow along the *c*-axis direction [19,23]. As shown in Fig. 1d, the SAED pattern was recorded on a single nanowire. Evidently, the CdS nanowire is a single crystal of hexagonal CdS, and the bright diffraction spots are indicative of its high crystallinity from Fig. 1d. Moreover, the SAED pattern can be indexed for the [0001] zone axis of hexagonal CdS, also indicating that preferential growth may occur along its *c*-axis direction. Fig. 1e shows the diameter distribution at the count of about 100 CdS nanowires. It is obvious that the diameters of the CdS nanowires are in the range of 24–30 nm and the average diameter of the CdS nanowires is about 26 nm, demonstrating that the CdS nanowires are of high uniform diameter. In this hydrothermal reaction, ethylenediamine(en) acts as a solvent as well as a complexing agent. At first, cadmium ions could combine with an ethylenediamine molecule (which acts as a bidentate ligand) to form a Cd–ethylenediamine complex ($[Cd(en)_2]^{2+}$) [12], which is stabilized in the solution. Meanwhile, S powder was dissolved in ethylenediamine. Finally, due to the slow release of S^{2-} ions and the low free Cd^{2+} concentration ($\log \beta_2 = 10.09$, β_2 is the stability constant of the complex $[Cd(en)_2]^{2+}$), the reaction rate is slow, which is in favor of the orientated growth of the CdS nanowires [19].

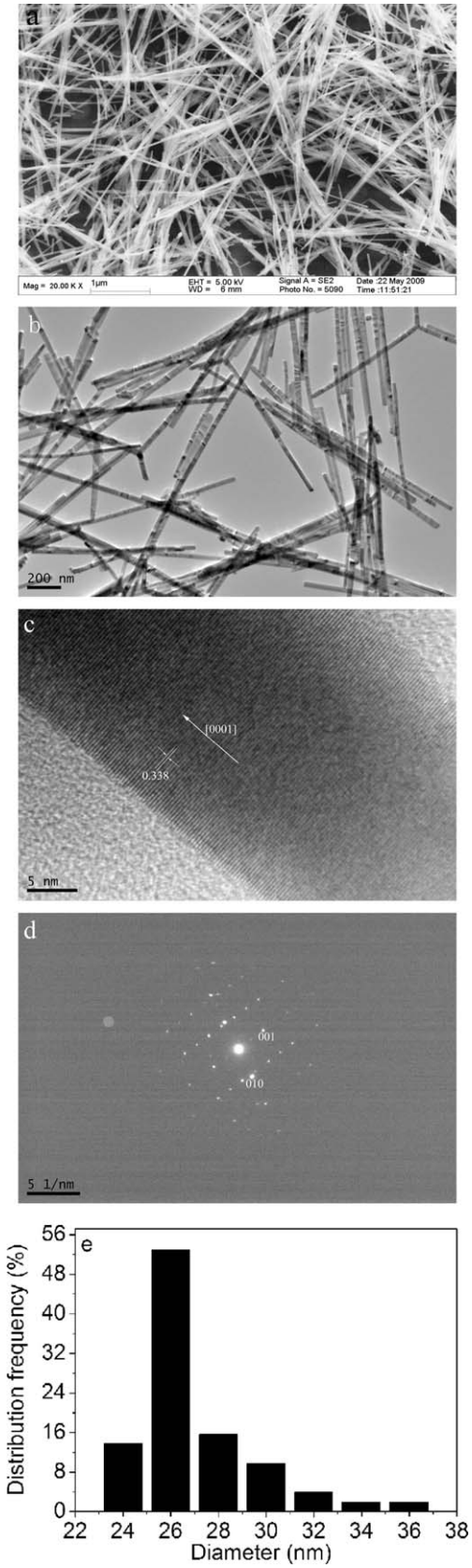

Fig. 1. FESEM image (a), TEM image (b), HRTEM image (c), its SAED pattern (d) and diameter distribution (e) of the as-prepared CdS nanowires.

UV–vis absorption spectroscopy is one of the most widely used techniques for optical characterization of nanomaterials. Fig. 2a shows the representative UV–vis absorption spectra of the CdS

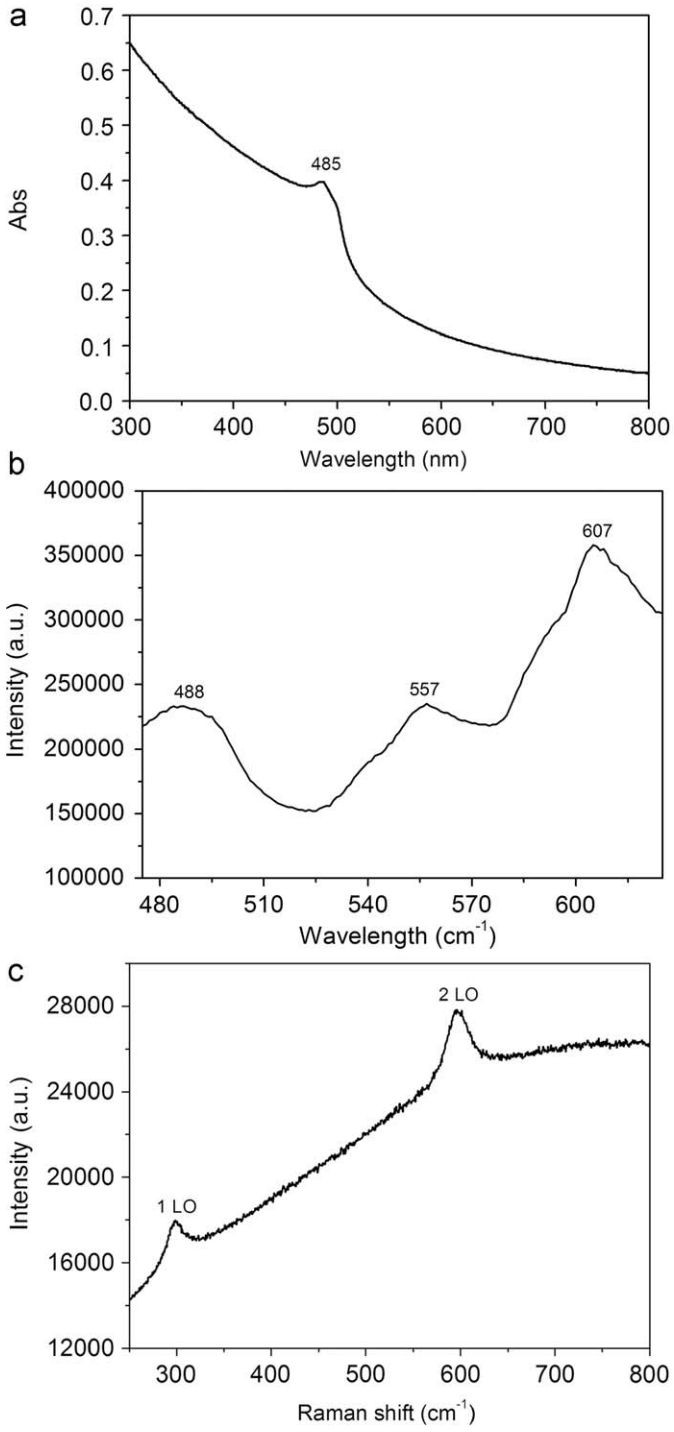

Fig. 2. Optical absorption spectrum (a), PL spectrum (b) and Raman spectrum (c) of the CdS nanowires.

nanowires dispersed in the anhydrous ethanol solution at room temperature. The samples were well dispersed in anhydrous ethanol to form a suspension. There is an adsorption band peaked at ~485 nm present in Fig. 2a, which is assigned to the first excitation of CdS. The band gap of as-prepared CdS nanowires is estimated to be ~2.56 eV from the UV–vis absorption spectra [19]. This value is larger than the reported value 2.42 eV of bulk CdS (512 nm) [24,25]. The obvious blue-shift (27 nm) to short wavelength is due to the quantum confinement effect of the small diameter. Moreover, the sharp edge of absorption spectrum can be ascribed to size uniformity of the nanowires. This conclusion is consistent with the above statistical result shown in Fig. 1d. PL is also acquired to determine the optical properties of the CdS nanowires. Fig. 2b shows PL spectrum of the as-prepared CdS nanowires with 350 nm excitation under the room temperature. It displays three distinct emission bands that are a blue emission band at 488 nm, a yellow emission one at 557 nm and a yellow emission one at 607 nm shown in Fig. 2b. The second emission band might be assigned to the electron–hole recombination of CdS, the first peak may correspond to the near band edge emission, and the final peak may be attributed to surface emission and possible metal vacancies. Similar band edge emission was also reported on previous CdS nanoribbons [5]. Raman spectroscopy is a powerful tool for the investigation of the doping concentration, lattice defect identification, and crystal orientation properties of the materials. Fig. 2c displays the room-temperature Raman spectra of the CdS nanowires excited by the 514.5 nm line of an Ar^+ laser. The Raman peaks were analogous to the pure crystalline CdS. The peaks at 298.6 and 597.7 cm^{-1} correspond to the first-order (1LO) and the second-order (2LO) longitudinal optical phonon modes of CdS, which are polarized in the *x*–*z* face and strongly coupled to the exciton along *c*-axis, respectively [26–29]. From the Raman spectra, it is interestingly found that the 2LO mode is stronger than the 1LO mode. Since the strength of exciton–phonon coupled in semiconductors can be assessed by the intensity ratio of overtone of phonon to the fundamental (I_{2LO}/I_{1LO}) [27,30,31]. The large intensity ratio of the NWs reflects a strong exciton–LO phonon because the phonon was confined in the transverse directions and the transfer of the elementary excitation (carriers, exciton, and phonon) in the longitudinal direction [32]. These single-crystal CdS nanowires possess good optical properties and may provide promising building blocks for photonic devices.

The electrical transport properties of single CdS NW were studied *in situ* inside a TEM using a Nanofactory TEM microscope sample holder. The vacuum level of the TEM was about 2×10^{-5} Pa. The bottom W (tungsten) electrode (Fig. 3a) was stationary and the top sharp W tip was movable via control of a piezotube. Firstly, the nanoprobe was moved to contact with a single NW. The corresponding TEM image and *I*–*V* curve were obtained shown in Fig. 3a and b, respectively. The *I*–*V* curve shows an almost symmetric non-ohmic contact behavior resulting from the back-to-back Schottky contacts formed between the tungsten nanoprobe and the single CdS NW. Zhang et al. have suggested a metal–semiconductor–metal (*M*–*S*–*M*) model to analyze quantitatively the *I*–*V* characteristics of such a *M*–*S*–*M* system [21,22]. Based on this model, we can reproduce the observed *I*–*V* characteristics using a few fitting variables, and estimate the intrinsic parameters of the single CdS NW.

The schematic diagram of the *M*–*S*–*M* structure and its equivalent circuit is shown in Fig. 3c. From Fig. 3c, the voltages on barrier 1, the nanowire and barrier 2 are denoted as V_1, V_{NW} and V_2 respectively, we finally get

$$V = V_1 + V_{NW} + V_2 \tag{1}$$

At low bias (for example <0.5 V), the total voltage is distributed mainly on the two Schottky Barriers, i.e., V_1, $V_2 \gg V_{NW}$. Particularly, the voltage drop on the reverse-biased Schottky barrier 1 increases rapidly and becomes dominating until about 5 V when the current begins to become notable, in the meanwhile the voltage on the nanowire becomes non-negligible. At the same time, the voltage drop across the forward-biased Schottky barrier 2 remains small. In the intermediate bias, the reverse-biased Schottky barrier dominates total current *I* as follow [21]:

$$\ln I = \mathrm{Ln}(SJ) = \ln S + V\left(\frac{q}{kT} - \frac{1}{E_0}\right) + \ln J_s \tag{2}$$

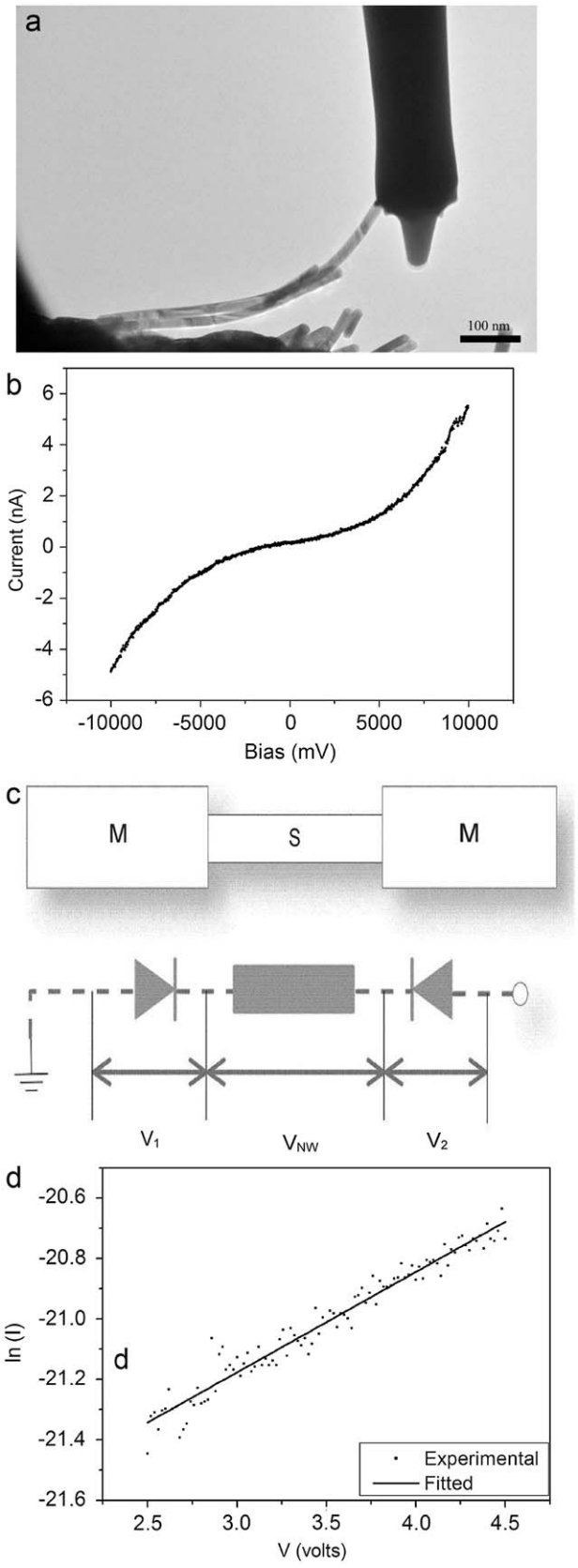

Fig. 3. (a) TEM image of the single CdS NW and the measured electrodes, (b) the *I–V* curve of the single CdS NW, (c) schematic diagram of the *M–S–M* structure and its equivalent circuit and (d) experimental and fitted plots of ln(*I*) vs. *V* for the CdS NW at intermediate bias in Fig. 3b.

where J is the current density through the Schottky barrier, S is the contact area associated with this barrier, and for simplicity the contact area is assumed to the cross-sectional area of the nanowire. E_0 is a parameter that depends on the carriers density, and J_s is a slowly varying function of applied bias. The plot (ln I vs. V) is shown in Fig. 3d. From Fig. 3d, we can obtain the E_0 ($E_0 = 26.30$ meV) from the slope of the fitted straight line. The charge carrier concentration N_d (electron concentration $n = N_d$) can be calculated as follows [20]:

$$E_0 = E_{00}\coth\left(\frac{qE_{00}}{kT}\right) \tag{3}$$

$$E_{00} = \frac{h}{4\pi}\left[\frac{N_d}{m_n^*\varepsilon_s\varepsilon_0}\right]^{1/2} \tag{4}$$

where E_{00} is a very important parameter in tunneling theory, N_d is the donor density at the metal/semiconductor interface, m_n^* is the effective mass of electron, ε_s is the relative permittivity of the semiconducting nanowire and ε_0 is the permittivity of free space.

At larger bias, the voltage drop V_1 across this barrier starts to saturate and the thickness reduction of Schottky barrier 1 for electron tunneling becomes less effective. The voltage V_{NW} on the nanowire increases almost linearly with the bias and becomes the dominating term at $V > 20$ V (The figure for V_{NW} on the nanowire is not given here.). In this large bias regime, the *I–V* curve can be differentiated to obtain the resistance of the nanowire directly:

$$R = \frac{dV_{NW}}{dI} \approx \frac{dV}{dI} \tag{5}$$

From this equation, the resistance of single CdS nanowire was determined to be 31.18 MΩ extracted from the *I–V* curve at large bias. The electron mobility can be obtained using the equation $\mu = 1/(nq\rho)$ combining with Eqs. (3)–(5), where ρ is the resistivity of the nanowire. Application of this procedure to Fig. 3b, the fitted values of resistivity, electron concentration and electron mobility of the CdS NW are 0.43 Ω cm, 2.3×10^{17} cm^{-3} and 62.83 cm^2 V^{-1} s^{-1}, respectively.

4. Conclusions

In conclusion, we have demonstrated a rapid and convenient hydrothermal method for the preparation of one-dimensional CdS nanowires with high uniformity and high yield. The as-prepared CdS nanowires have average 26 nm in diameter and length up to several micrometres. The direct band gap of the CdS nanowires is ~2.57 eV calculated by the UV–vis absorption spectra. PL and Raman optical characterizations of the CdS NWs reveal their good optical as well as excellent crystalline qualities. Furthermore, the values of resistivity, electron concentration and electron mobility of a single CdS NW are 0.43 Ω cm, 2.3×10^{17} cm^{-3} and 62.83 cm^2 V^{-1} s^{-1} with the metal–semiconductor–metal model, respectively. This simple synthesis methodology together with the good optical and electronic properties makes this material scientifically and technologically interesting.

Acknowledgments

This work was financially supported by the National Basic Research Program of China (973 Program: 2007CB936300), NSFC (No. 20875014), FANEDD (No. 200053), 2008DFA51180 and the

Scientific Research Foundation of Graduate School of Southeast University.

References

[1] A.M. Morales, C.M. Liber, Science 279 (1998) 208.
[2] Z.W. Pan, Z.R. Dai, Z.L. Wang, Science 291 (2001) 1947.
[3] W.U. Huynh, J.J. Dittmer, A.P. Alivisatos, Science 295 (2002) 2425.
[4] X. Duan, C. Niu, V. Sahi, J. Chen, J.W. Parce, S. Empedocles, J.L. Goldman, Nature 425 (2003) 274.
[5] Y.K. Liu, J.A. Zapien, C.Y. Geng, Y.Y. Shan, C.S. Lee, S.T. Lee, Appl. Phys. Lett. 85 (2004) 3241.
[6] J. Zhang, F. Jiang, L. Zhang, J. Phys. Chem. B 108 (2004) 7002.
[7] Y.F. Lin, J.H. Song, Y. Ding, S.Y. Lu, Z.L. Wang, Appl. Phys. Lett. 92 (2008) 022105.
[8] Y.F. Lin, J.H. Song, Y. Ding, S.Y. Lu, Z.L. Wang, Adv. Mater. 20 (2008) 3127.
[9] X.F. Duan, C.M. Lieber, Adv. Mater. 12 (2000) 298.
[10] C. Ye, G. Meng, Y. Wang, Z. Jiang, L. Zhang, J. Phys. Chem. B 106 (2002) 10338.
[11] Q. Nie, Z. Xu, Q. Yuan, G. Li, Mater. Chem. Phys. 82 (2003) 808.
[12] J.S. Jang, U.A. Joshi, J.S. Lee, J. Phys. Chem. C 111 (2007) 13280.
[13] H.M. Wang, P.F. Fang, Z. Chen, S.J. Wang, J. Alloys Compd. 461 (2008) 418.
[14] J. Puthussery, A.D. Lan, T.H. Kosel, M. Kuno, ACS Nano 2 (2008) 357.
[15] D. Wang, J.G. Lu, C.J. Otten, W.E. Buhro, Appl. Phys. Lett. 83 (2003) 5280.
[16] Y. Cui, X.F. Duan, J.T. Hu, C.M. Lieber, J. Phys. Chem. B 104 (2000) 5213.
[17] D. Zhang, C. Li, S. Han, X. Liu, T. Tang, W. Jin, C. Zhou, Appl. Phys. Lett. 82 (2003) 112.
[18] S.M. Sze, D.J. Coleman, A. Loya, Solid-State Electron. 14 (1971) 1209.
[19] Q.Q. Wang, G. Xu, G.R. Han, J. Solid State Chem. 178 (2005) 2680.
[20] F.A. Padovani, R. Stratton, Solid-State Electron. 9 (1966) 695.
[21] Z.Y. Zhang, C.H. Jin, X.L. Liang, Q. Chen, L.M. Peng, Appl. Phys. Lett. 88 (2006) 073102.
[22] Z.Y. Zhang, K. Yao, Y. Liu, C.H. Jin, X.L. Liang, Q. Chen, L.M. Peng, Adv. Funct. Mater. 17 (2007) 2478.
[23] Y.F. Lin, Y.J. Hsu, W.Y. Cheng, S.Y. Lu, Chem. Phys. Chem. 110 (2009) 711.
[24] J. Butty, N. Peyghambarian, Y.H. Kao, J.D. Mackenzie, Appl. Phys. Lett. 69 (1996) 3224.
[25] S. Kar, S. Chaudhuri, J. Phys. Chem. B 110 (2006) 4542.
[26] Y.W. Wang, G.W. Meng, L.D. Zhang, C.H. Liang, J. Zhang, Chem. Mater. 14 (2002) 1773.
[27] A.L. Pan, R.B. Liu, Q. Yang, Y.C. Zhu, G.Z. Yang, B.S. Zou, K.Q. Chen, J. Phys. Chem. B 109 (2005) 24268.
[28] S.P. Mondal, K. Das, A. Dhar, S.K. Ray, Nanotechnology 18 (2007) 095606.
[29] C.A. Arguello, D.L. Rousseau, S.P.S. Porto, Phys. Rev. 181 (1969) 1351.
[30] J.J. Shiang, S.H. Risbud, A.P. Alivisatos, J. Chem. Phys. 98 (1993) 8432.
[31] W.Z. Shen, Physica B 322 (2002) 201.
[32] B.L. Cao, Y. Jiang, C. Wang, W.H. Wang, L.Z. Wang, M. Niu, W.J. Zhang, Y.Q. Li, S.T. Lee, Adv. Funct. Mater. 17 (2007) 1501.